Twilight Irradiance Reflected by the Earth Estimated from Clouds and the Earth's Radiant Energy System (CERES) Measurements

SEIJI KATO AND NORMAN G. LOEB

Center for Atmospheric Sciences, Hampton University, Hampton, Virginia

12 August 2002 and 16 January 2003

ABSTRACT

The upward shortwave irradiance at the top of the atmosphere when the solar zenith angle is greater than 90° (twilight irradiance) is estimated from radiance measurements by the Clouds and the Earth's Radiant Energy System (CERES) instrument on the Tropical Rainfall Measuring Mission (TRMM) satellite. The irradiance decreases with solar zenith angle from 7.5 W m^{-2} at 90.5° to 0.6 W m^{-2} at 95.5°. The global and daily average twilight irradiance is 0.2 W m^{-2}, which is three orders of magnitude smaller than the daily and global average reflected irradiance at the top of the atmosphere. Therefore, the twilight irradiance can be neglected in global radiation budget estimate. The daily average twilight irradiance, however, can be more than 1 W m^{-2} at polar regions during seasons when the sun stays just below the horizon for a long period of time.

1. Introduction

When standing outside after sunset, one notices that there is appreciable visible light for a while before the sky is dark enough to see stars. When flying on an airplane, one also notices that there is enough skylight to identify solar illuminated clouds well after the sun appears to have set at the surface. While these phenomena are common to us, the twilight irradiance is usually neglected in earth radiation budget estimation (e.g., Young et al. 1998).

According to Rozenberg (1966), the term ''twilight'' refers to the entire complex of optical phenomena that occur in the atmosphere when the sun is approximately within 5°–10° of the horizon. In this study, the twilight irradiance is defined as the upward shortwave irradiance at the top of the atmosphere when the solar zenith angle is greater than 90°. The purpose of this study is to estimate the twilight irradiance and to determine if it is small compared to the global and daily average reflected shortwave irradiance. For the estimate, we use radiances measured by the Clouds and the Earth's Radiance Energy System (CERES; Wielicki et al. 1996) instrument on the Tropical Rainfall Measuring Mission (TRMM) satellite (Kummerow et al. 1998).

Corresponding author address: Dr. Seiji Kato, Mail Stop 420, NASA Langley Research Center, Hampton, VA 23681-2199.
E-mail: s.kato@larc.nasa.gov

2. CERES data

Since we are interested in the average irradiance, measured radiances are sorted into solar zenith, viewing zenith, and viewing azimuth angle bins, and the average radiance at each angular bin is determined. These average radiances are then integrated over viewing zenith and azimuth angles to obtain the irradiance as a function of the solar zenith angle. A schematic diagram of the geometry is shown on Fig. 1. The position of the CERES instrument S_1 is defined by the colatitude angle Θ, longitude angle Φ, and distance from the center of the earth $R + h$, where R is the radius of the earth and h is the height of the instrument from the surface of the earth (Geier et al. 2002). The height h of the CERES instrument on the TRMM satellite is approximately 350 km. In a spherical geometry, the viewing zenith angle θ depends on the altitude where it is defined. The viewing zenith angle of a tangential path to the earth's surface θ_t is approximately 71° when the viewing zenith angle is defined at 350 km above the surface, and 80° when it is defined at 100 km. The CERES instrument scans the earth from 79° zenith angle (defined at 350 km) passing the nadir to either 56° (short scan) or 79° (normal scan) with a speed of 63.5° s^{-1}. The viewing azimuth angle ϕ is defined relative to the sun such that the azimuth angle of the position of the sun is always 180°.

When $\theta < \theta_t$, the earth's surface intercepts the line of sight of the instrument, and more than half of the

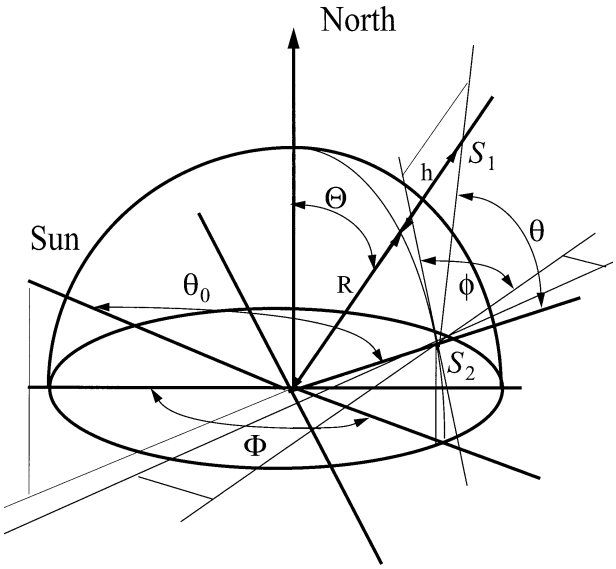

FIG. 1. Schematic diagram of the CERES instrument position and viewing geometry. The position of the satellite is at S_1 and the center of the footprint is at S_2. The satellite position is expressed by the colatitude Θ, longitude Φ, and distance from the center of the earth $R + h$. Here θ, ϕ, and θ_0 are the viewing zenith angle defined at the surface, viewing azimuth angle, and solar zenith angle, respectively.

field of view of the CERES instrument is subtended by the earth. The field of view of the CERES instrument projected on the earth's surface (footprint) varies depending on the viewing zenith angle. The size of a CERES footpoint at nadir is approximately 10 km. The solar zenith angle θ_0 over a CERES footpoint is defined at the surface when $\theta < \theta_t$. When $\theta > \theta_t$, however, θ_0 is difficult to define because earth does not intercept the line of sight of the instrument. Because the upward irradiance at the top of the atmosphere after sunset as observed at the surface is at issue, θ_0 over a footprint for viewing zenith angles greater than θ_t is assumed to be the same as that of a footpoint at θ_t for the same scan of the CERES instrument.

Since the radiance depends on the viewing azimuth angle ϕ, radiances at all azimuth angles need to be known. As ϕ decreases and approaches zero, however, the sun enters the field of view of the CERES instrument. In order to avoid the sun in its field of view, the CERES instrument does not measure the radiance when the viewing angle is in orbital solar avoidance zones, which includes both sides of nadir. As a consequence, under the CERES normal-scan mode, measured radiances are not available at the azimuth angle less than 30° and greater than 150° when the solar zenith angle is between 85° and 110°. Even though the direct solar irradiance needs to be excluded from the twilight irradiance estimate, radiances at small azimuth angles cannot be neglected completely. This causes a problem in estimating azimuthally averaged radiances for a given viewing zenith angle and solar zenith angle. In order to demonstrate the sensitivity to the assumption used to determine radiances at angles that were not measured, we used two different methods to estimate the azimuthally averaged radiance. The first method is simply taking an arithmetic average of measured radiances without explicitly sorting them into azimuth angle bins. The second method involves averaging radiances sorted into 5° azimuth angle bins. We used the averaged radiance at 30° (150°) azimuth angle for radiances at azimuth angles smaller than 30° (greater than 150°). The first method weights azimuth angles depending on measurement frequency of each angle for the average while the second method weights all azimuth angles equally.

Radiances measured by the CERES instruments are wavelength-dependent power detected by the instrument divided by the solid angle of its field of view and surface area of the detector. The CERES instrument measures shortwave radiation from 0.2 to 5 μm (Loeb et al. 2001). Because the response of the CERES instrument varies spectrally, the radiance measured by the instrument is weighted by its spectral response. The effect of the response function needs to be eliminated to account for the entire spectrum of shortwave radiation reflected by the earth. Because the radiance spectrum reflected by the earth depends on the scene type, Loeb et al. (2001) used scene-dependent coefficients to convert radiances weighted by the CERES instrument spectral response function (filtered radiance) to radiances detected without the spectral response function (unfiltered radiance). Their unfiltered shortwave radiances, however, are unavailable when the solar zenith angle is greater than 90° or when the viewing zenith angle is large because imager data that provide scene identification for footprints are not available.

Therefore, we need to establish coefficients to convert filtered radiance to unfiltered radiances for our purpose. Following Loeb et al. (2001), radiances reflected by the earth were first computed at the solar zenith angle greater than 90° using the MODTRAN radiative transfer code (Kneizys et al. 1988). Second, wavelength-dependent modeled radiances were weighted by the spectral response function of the CERES instrument to obtain filtered radiances. Third, filtered radiances were weighted by the point spread function of the CERES instrument to simulate measured radiances as a function of viewing zenith and azimuth angles and solar zenith angles. Fourth, relations between unfiltered and filtered radiances were obtained by fitting the unfiltered radiances using

$$I_{uf} = c_0 + c_1 I_f + c_2 I_f^2, \quad (1)$$

where I_f and I_{uf} are the filtered and unfiltered radiance, respectively. The coefficients c_0, c_1, and c_2 were obtained as a function of solar zenith angle by least squares fitting. We considered two types of atmosphere to determine the coefficients by MODTRAN, a molecular atmosphere and atmosphere with a thick cloud extending 1–10 km. Since the air mass is about 40 at the surface for a tangential path to the surface of the earth (Roz-

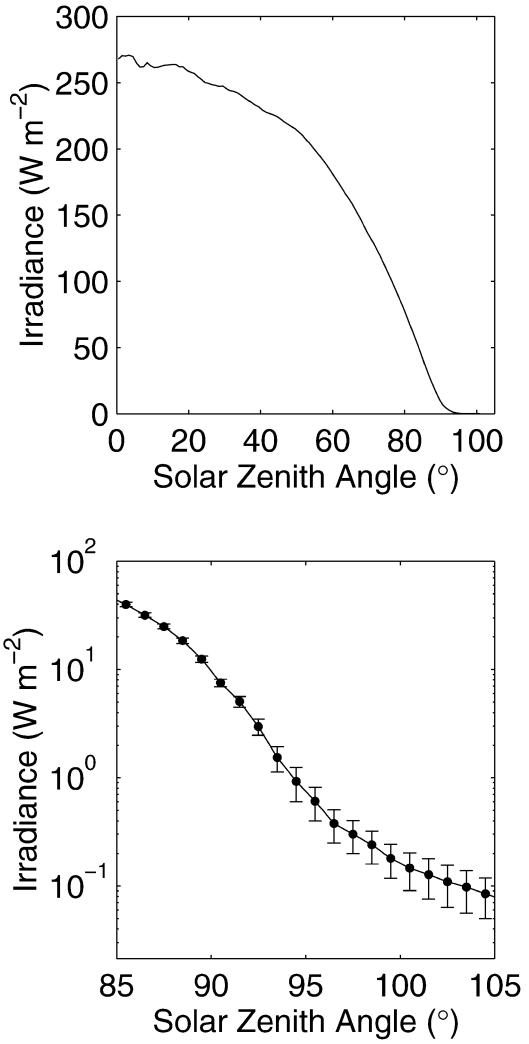

FIG. 2. Average irradiance integrated from radiances measured by the CERES instrument for the solar zenith angle from (top) 0° to 105° and (bottom) 85° to 105°. CERES data taken from Jan 1998 to Aug 1998 and Mar 2000 for all scene types were used for the computation. Two different methods for the estimate provide the error bars.

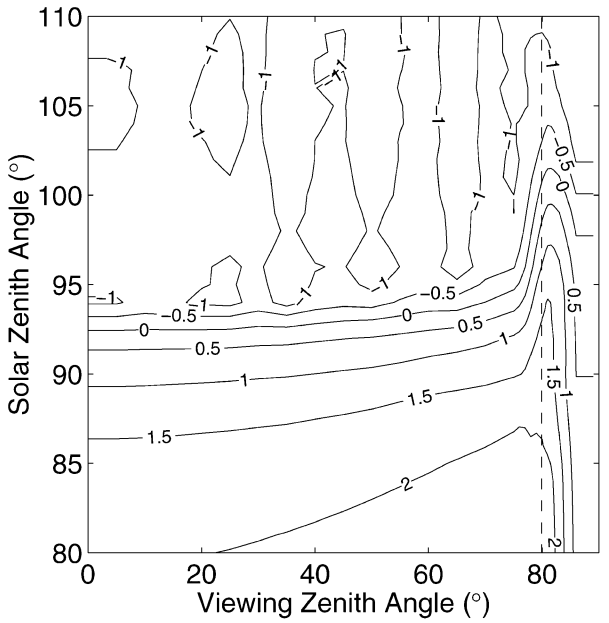

FIG. 3. Contour plot of logarithm (base 10) of the azimuthally averaged radiance derived from radiance measurements by the CERES instrument on the TRMM satellite. The viewing zenith angle is computed at 100 km above the surface. The dashed line indicates the viewing zenith angle of the tangential path to the surface of the earth.

enberg 1966), the optical thickness of a molecular atmosphere is about 3.6 at 560 nm for the tangential path. Therefore, the surface albedo of the earth does not affect the modeled radiance very much; we assumed the surface albedo to be 0.3 in the model.

3. Results and discussion

Figure 2 shows the irradiance as a function of solar zenith angle obtained from measured radiances by the CERES instrument for all scene types. Measured radiances between 40°N and 40°S from January 1998 to August 1998 and March 2000 were used. The twilight irradiance given by the simple arithmetic average described in the previous section, F_{ar}, is 6.9 W m^{-2} at 90.5° and 0.4 W m^{-2} at 95.5°. The twilight irradiance F_{az} given by the second method that fills empty bins by measured radiances taken at the closest azimuth angle is 8.1 W m^{-2} at 90.5° and 0.8 W m^{-2} at 95.5°. Note that these twilight irradiances are converted to the 20-km reference altitude from the satellite altitude by scaling irradiances inversely proportional to the square of the distance from the center of the earth as discussed by Loeb et al. (2002). The error bar shown in Fig. 2 is based on these two estimates of the twilight irradiance. The error bar, therefore, indicates the uncertainty in estimating the average twilight irradiance from the CERES radiance measurements; it is not the envelope of the variation of twilight irradiances. As the solar zenith angle of the sun increases, the sun only illuminates a higher portion of the atmosphere. Because the scattering coefficient decreases with height, the twilight irradiance decreases with increasing altitude of the atmosphere illuminated by the sun.

Figure 3 shows unfiltered azimuthally averaged radiances from CERES measurements as a function of solar zenith angle and viewing zenith angle. The main contribution to the twilight irradiance comes from radiances at viewing zenith angle greater than θ_t. The azimuthally averaged radiance has a maximum at the zenith angle at θ_t when the solar zenith angle is about 85°. The maximum moves toward the larger viewing zenith angle with increasing the solar zenith angle because the earth casts a shadow on the line of sight of the CERES instrument when the altitude h of a point on the line of sight is less than $\approx R\ (1/\sin\theta_0 - 1)$ if

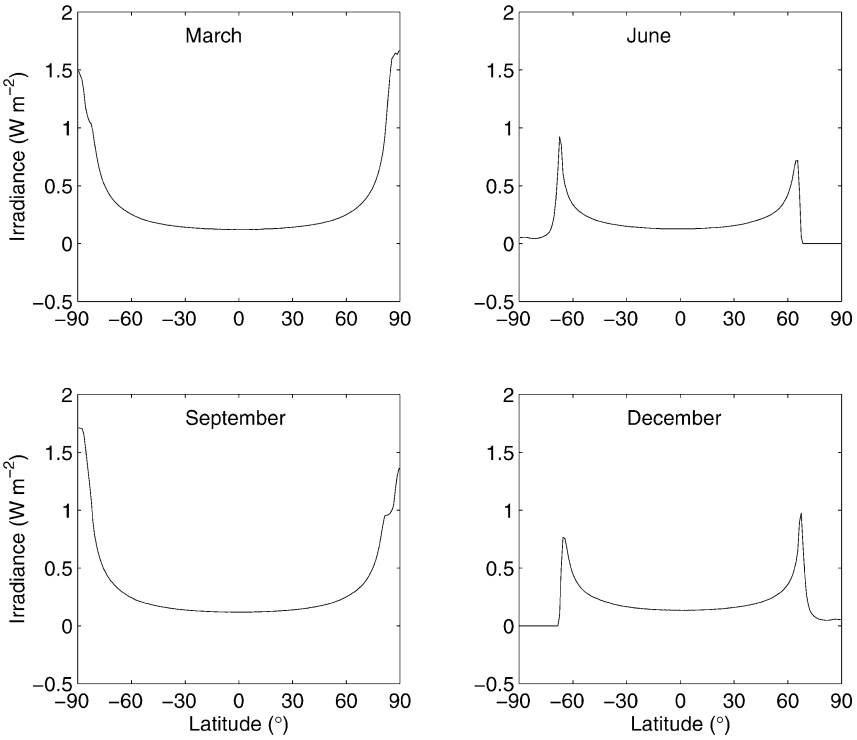

FIG. 4. Daily average twilight irradiance as a function of latitude. The relation between the irradiance and solar zenith angle shown in Fig. 2 is used to compute the daily average twilight irradiance. The positive latitude indicates the Northern Hemisphere.

refraction is neglected. As θ_0 increases and the shadow extends to a higher part of the atmosphere, a larger part of the line of sight for the viewing zenith angle greater than θ_t is in the shadow. Therefore, a larger part of the field of view is subtended by the shadow. When this twilight period is observed from the surface, one can also see that the boundary between the illuminated sky and the shadowed sky rises as the sun sets on a clear day, while the brightness and hue of the sky changes with the solar zenith angle (Minnaert 1954, 268–275; Greenler 1980, 131–132).

The twilight irradiances estimated by two methods, F_{ar} and F_{az}, differ by 14% at the solar zenith angle of 90.5° and 50% at 95.5° relative to F_{az}. If radiances at the viewing azimuth angle less than 30° are completely neglected and fill these bins with 0 value to compute F_{az}, the irradiance reduces by 33% and 90% at the solar zenith angle of 90.5° and 95.5°, respectively. We also altered the size of the azimuth angle bin from 5° to 1°; it increases F_{az} by 0.5% at 90.5° solar zenith angle and decreases by 12% at 95.5° solar zenith angle. These changes are caused by the noisier average radiances because less samples are in 1° azimuth bins than 5° bins. Therefore, the error in the estimate irradiance is mainly caused by the assumption of radiances at viewing azimuth angle less than ≈30°. The error could be large depending on the assumption. In addition, converting filtered radiances to unfiltered radiances introduces error. The global and daily averaged F_{ar} and F_{az} are 0.16 and 0.22 W m^{-2}, respectively. Therefore, the global and daily average twilight irradiance is three orders of magnitude smaller than the daily and global average reflected irradiance of 107 W m^{-2} at the top of the atmosphere (Kiehl and Trenberth 1997). Consequently, the twilight irradiance can be neglected in global radiation balance computations. The twilight irradiance, however, might be significant compared to the reflected irradiance over the regions where the average solar zenith angle is large. To demonstrate this point, Fig. 4 shows the daily average twilight irradiance as a function of latitude for four selected months. The irradiance as a function of solar zenith angle shown by Fig. 2 is assumed to be independent of the location so that the daily average twilight irradiance depends only on day of year and latitude. Note that the asymmetry around the equator for March and September is caused by the lack of symmetry with the equinoxes in both months. We included the variation of the distance between the sun and earth in the estimate. However, it causes a negligible variation in the global and daily average twilight irradiance (≈0.01 W m^{-2}). As shown on the figure, the daily average twilight irradiance can be more than 1 W m^{-2} at polar regions where the sun stays just below the horizon for a long time period. Therefore, contribution of the twilight irradiance to the regional or zonally averaged reflected irradiance can be significant in polar regions.

Acknowledgments. We thank Mr. B. A. Wielicki, Dr. T. P. Charlock, and D. F. Young of NASA Langley Research Center for useful discussions, and Mr. P. C. Hess of Science Applications International Corporation and Dr. K. J. Priestley of NASA Langley Research Center for providing CERES instrument information. The work is supported by the CERES project under NASA Grant NAG-1-2318.

REFERENCES

Geier, E. B., R. N. Green, D. P. Kratz, P. Minnis, W. Miller, S. K. Nolan, and C. B. Franklin, cited 2002: Clouds and Earth's Radiant Energy System single satellite footprint TOA/surface flux and clouds (SSF) collection document. 243 pp. [Available online at http://asd-www.larc.nasa.gov/ceres/collect_guide/.]

Greenler, R., 1980: *Rainbows, Halos, and Glories.* Cambridge University Press, 195 pp.

Kiehl, J. T., and K. E. Trenberth, 1997: Earth's annual global mean energy budget. *Bull. Amer. Meteor. Soc.,* **78,** 197–208.

Kneizys, F. X., E. P. Shettle, L. W. Abreu, J. H. Chetwynd, G. P. Anderson, W. O. Gallery, J. E. A. Selby, and S. A. Clough, 1988: Users guide to LOWTRAN 7. Air Force Geophysics Laboratory Tech. Rep. AFGL-TR-88-0177, 137 pp.

Kummerow, C., W. Barnes, T. Kozu, J. Shiue, and J. Simpson, 1998: The Tropical Rainfall Measuring Mission (TRMM) sensor package. *J. Atmos. Oceanic Technol.,* **15,** 809–817.

Loeb, N. G., K. J. Priestley, D. P. Kratz, E. B. Geire, R. N. Green, B. A. Wielicki, P. O. Hinton, and S. K. Nolan, 2001: Determination of unfiltered radiances from the Clouds and the Earth's Radiant Energy System instrument. *J. Appl. Meteor.,* **40,** 822–835.

——, S. Kato, and B. A. Wielicki, 2002: Defining top-of-the-atmosphere flux reference level for earth radiation budget studies. *J. Climate,* **15,** 3301–3309.

Minnaert, M., 1954: *The Nature of Light and Color in the Open Air.* Dover, 361 pp.

Rozenberg, G. V., 1966: *Twilight: A Study in Atmospheric Optics.* Plenum Press, 358 pp.

Wielicki, B. A., B. R. Barkstrom, E. F. Harrison, B. B. Lee III, G. Louis Smith, and J. E. Cooper, 1996: Clouds and the Earth's Radiant Energy System (CERES): An earth observing system experiment. *Bull. Amer. Meteor. Soc.,* **77,** 853–868.

Young, D. F., P. Minnis, D. R. Doelling, G. G. Gibson, and T. Wong, 1998: Temporal interpolation methods for the Cloud and the Earth's Radiant Energy System (CERES) experiment. *J. Appl. Meteor.,* **37,** 572–590.